Crystal Structure of Human Cytosolic 5′-Nucleotidase II
INSIGHTS INTO ALLOSTERIC REGULATION AND SUBSTRATE RECOGNITION*

Karin Walldén[‡§], **Pål Stenmark**[¶], **Tomas Nyman**[¶], **Susanne Flodin**[¶], **Susanne Gräslund**[¶], **Peter Loppnau**[∥], **Vera Bianchi**[**], and **Pär Nordlund**[§¶1]

From the [‡]Department of Biochemistry and Biophysics, Stockholm University, 10691 Stockholm, Sweden, the [¶]Structural Genomics Consortium, Karolinska Institutet, 17177 Stockholm, Sweden, the [∥]Structural Genomics Consortium, University of Toronto, Toronto, Ontario M5G 1L5, Canada, the [**]Department of Biology, University of Padova, I-35131 Padova, Italy, and the [§]Department of Medical Biochemistry and Biophysics, Karolinska Institutet, 17177 Stockholm, Sweden

Cytosolic 5′-nucleotidase II catalyzes the dephosphorylation of 6-hydroxypurine nucleoside 5′-monophosphates and regulates the IMP and GMP pools within the cell. It possesses phosphotransferase activity and thereby also catalyzes the reverse reaction. Both reactions are allosterically activated by adenine-based nucleotides and 2,3-bisphosphoglycerate. We have solved structures of cytosolic 5′-nucleotidase II as native protein (2.2 Å) and in complex with adenosine (1.5 Å) and beryllium trifluoride (2.15 Å). The tetrameric enzyme is structurally similar to enzymes of the haloacid dehalogenase (HAD) superfamily, including mitochondrial 5′(3′)-deoxyribonucleotidase and cytosolic 5′-nucleotidase III but possesses additional regulatory regions that contain two allosteric effector sites. At effector site 1 located near a subunit interface we modeled diadenosine tetraphosphate with one adenosine moiety in each subunit. This efficiently glues the tetramer subunits together in pairs. The model shows why diadenosine tetraphosphate but not diadenosine triphosphate activates the enzyme and supports a role for cN-II during apoptosis when the level of diadenosine tetraphosphate increases. We have also modeled 2,3-bisphosphoglycerate in effector site 1 using one phosphate site from each subunit. By comparing the structure of cytosolic 5′-nucleotidase II with that of mitochondrial 5′(3′)-deoxyribonucleotidase in complex with dGMP, we identified residues involved in substrate recognition.

Cytosolic 5′-nucleotidase II (cN-II),[2] also called purine 5′-nucleotidase, IMP-GMP specific nucleotidase or high K_m 5′-nucleotidase, is one of the seven known mammalian 5′-nucleotidases that catalyze the dephosphorylation of ribo- and deoxyribonucleoside monophosphates to nucleoside and inorganic phosphate (1, 2). The seven enzymes differ in substrate specificity, subcellular location, and tissue-specific expression. Intracellular 5′-nucleotidases regulate nucleotide levels by counteracting the action of nucleoside kinases and competing with other enzymes that use the nucleoside monophosphates. This complex network of interactions contributes to maintain nucleotide pools in tune with the metabolic needs of the cell (1, 2).

The structures of two of the six human intracellular 5′-nucleotidases, *i.e.* mitochondrial 5′(3′)-deoxyribonucleotidase (mdN) (3) and cytosolic 5′-nucleotidase III (cN-III) (PDB entry 2CN1) are known. The latter is almost identical to the published structure of mouse cN-III (4). Both mdN and cN-III belong to the haloacid dehalogenase (HAD) superfamily, which is defined by an α/β-Rossmann-like domain and a smaller 4-helix bundle domain, which, however, is not present in all HAD superfamily enzymes. The intracellular 5′-nucleotidases share three conserved motifs that have been found in HAD superfamily enzymes such as phosphoserine phosphatase (5) and β-phosphoglucomutase (6). The three motifs, Motif I (DXDX[T/V]L), Motif II ([T/S]), and Motif III (K(X$_x$)D(X)$_{0-4}$D), are located in the α/β-Rossmann-like domain and build up the catalytic phosphate-binding site in these enzymes. Motif I is directly involved in the reaction mechanism of 5′-nucleotidases (3), in which the first Asp makes a nucleophilic attack on the phosphate of the nucleoside monophosphate and the second Asp donates a proton to the leaving nucleoside. The mechanism is believed to involve both a pentavalent substrate intermediate (7) and a phosphoenzyme intermediate (6, 8). The similar composition of the phosphate-binding site among the structurally known HAD superfamily enzymes indicates that they have a similar catalytic mechanism for hydrolyzing

phosphomonoester bonds and suggests divergent evolution from a common progenitor. In both mdN and cN-III the active site is located in a cleft between the two domains (3, 4). In mdN, the smaller 4-helix bundle domain binds the base of the nucleotide and thereby determines the base specificity of the enzyme (3, 9).

The cN-II was first purified from chicken liver (10) and has been intensively investigated in vertebrates (11). As substrates it prefers the 6-hydroxypurine nucleoside monophosphates IMP, dIMP, GMP, dGMP, and XMP (10, 12–15) and functions as a tetramer (12, 16–18). It is ubiquitously expressed and is likely to play an important role in the regulation of purine nucleotide interconversions and in the regulation of IMP and GMP pools within the cell (1). The human enzyme was cloned in 1994 and predicted to be a 561 amino acid protein of 65 kDa (19), but it migrates on SDS-PAGE at a relative mass of 57 kDa (16, 20).

Unlike the other 5'-nucleotidases, cN-II is allosterically activated by adenine/guanine nucleotides, 2,3-bisphosphoglycerate (2,3-BPG) and adenine/guanine-based dinucleoside polyphosphates, *e.g.* diadenosine tetraphosphate (Ap4A) (12, 18). Of the nucleotides, the strongest activator is dATP followed by ATP (12), 2,3-BPG is as potent as ATP (12) and Ap4A is more potent than ATP (18, 21). The activation by ATP is dependent on the concentration of substrate and inorganic phosphate (12). The effectors ATP and Ap4A both lower the K_m and increase the V_{max} with IMP as substrate (12, 18). With GMP as substrate, Ap4A lowers the K_m whereas V_{max} is unaffected (18). The enzyme is also activated by millimolar concentrations of NaCl, KCl and LiCl (17). Addition of ATP and NaCl to the purified protein induces aggregation of the enzyme, whereas inorganic phosphate appears to have the opposite effect (16).

The enzyme also acts as a phosphotransferase, catalyzing the transfer of a phosphate from the monophosphate substrate to a nucleoside acceptor -preferentially inosine and deoxyinosine- to form a nucleoside monophosphate (22). Phosphate donors include any 6-hydroxypurine monophosphate substrate of the nucleotidase reaction (13–15, 22–24).

5'-Nucleotidases are likely to affect the phosphorylation level and the pharmacolgical activity of nucleoside analogs used in the treatment of cancer and viral diseases (1, 2). A number of studies have dealt with the possible role of cN-II in drug resistance (25–29). Purified recombinant human cN-II hydrolyzes the 5'-monophosphates of different purine and pyrimidine-based nucleoside analogs but shows negligible activity with cytosine-containing analogs (30). By its phosphotransferase activity, the enzyme phosphorylates the nucleoside analogs dideoxyinosine, tiazofuran, acyclovir, and ribavirin more efficiently than the cellular (deoxy)nucleoside kinases (23, 31). Increased cellular cN-II activity in Lesch-Nyhan syndrome might be associated with neurological symptoms related to this disease (32, 33).

Here we report three structures of human cN-II: native structure (2.2 Å), a complex with beryllium trifluoride (BeF$_3^-$) (2.15 Å) mimicking a transient phosphoenzyme intermediate, and a complex with two adenosines (1.5 Å) that enabled us to characterize two effector sites where we have modeled the effectors Ap4A and 2,3-BPG. All three structures have magnesium bound in the active site and 2– 6 sulfate ions bound, indicating possible binding sites for phospho-moieties of substrates and effectors. Furthermore, we identify residues that are most likely involved in substrate recognition.

EXPERIMENTAL PROCEDURES

Expression—Residues 1–536 of the 561-residue-long human cN-II were expressed in Rosetta2(DE) cells from the pET-based vector p28A-LIC. The expressed construct included an N-terminal His$_6$ tag and a thrombin protease cleavage site between the His tag and the protein. The presence and integrity of the sequence in the vector were confirmed by sequencing. Cells were grown at 37 °C and 225 rpm until A_{600} of 1.0 and then the temperature was reduced to 18 °C. After 50 min, expression of cN-II was induced by addition of isopropyl-β-D-thiogalactopyranoside to a concentration of 0.5 mM. Protein expression was allowed to continue over night at 18 °C. Harvested cells were resuspended in lysis buffer (50 mM HEPES pH 7.5, 500 mM NaCl, 10 mM imidazole, 10% glycerol and 0.5 mM TCEP) supplemented with one tablet of Complete EDTA-free protease inhibitor (Roche Applied Science) per 50 ml. 2000 units of benzonase was added, and the cells were disrupted by high pressure homogenization and centrifuged for 20 min at 40,000 × g.

Thermal Stability Shift Assay—Due to previous problems with precipitate formation during concentration of cN-II, we looked for a buffer in which cN-II is more soluble. To do this, we performed a thermal stability shift assay, in which the protein melting temperature was measured in 48 different buffers. A high melting temperature indicates that the protein is stable in the buffer. Fluorescence was measured from 20 to 89.6 °C, and the thermal stability shift was determined as described previously (34). The assay indicated that cN-II was more stable in phosphate-based than in HEPES-based buffers. Thus phosphate buffer was successfully used for further purification of cN-II. The thermal stability shift assay was run on an iCycler from Bio-Rad in a DNA- and RNase-free 96-well PCR plate. The total volume in each well was 25 μl with 10 μg of protein, 5 mM TCEP, SYPRO orange (Molecular Probes, Eugene, OR) diluted 5000× and buffer screen consisting of 48 different commonly used buffers.

Purification—The protein was purified using an ÄKTA-prime fast protein liquid chromatography instrument (GE Healthcare), with a 1-ml Ni^{2+}-charged His-Trap HP column (GE Healthcare) and a HiLoad 16/60 Superdex 200 gel filtration column (GE Healthcare). The His-Trap HP column was equilibrated in 50 mM HEPES, 500 mM NaCl, 10% glycerol, 10 mM imidazole, 0.5 mM TCEP, pH 7.5, and the His-tagged protein was eluted with the same buffer containing 250 mM imidazole. The fractions containing cN-II were pooled and applied onto the gel filtration column equilibrated in 50 mM sodium phosphate buffer, pH 7.4, 100 mM NaCl, 10% glycerol, 0.5 mM TCEP. The retention volume of cN-II corresponded to that of a tetramer. After purification, the protein was concentrated to 7.4 mg/ml. SDS-PAGE analysis shows a mass of 57 kDa similar to previous SDS-PAGE observations (16, 20), although the protein expressed here lacks the terminal 25 amino acids. Mass spectrometry (high performance liquid chromatography-electros-

TABLE 1
Crystallographic data collection and refinement statistics

	Native cN-II	cN-II-BeF$_3$	cN-II-adenosine
Data collection statistics			
Space group	I 2 2 2	I 2 2 2	I 2 2 2
Unit cell dimensions (Å)			
A	91.46	91.48	90.92
B	128.03	128.26	127.72
C	130.41	131.01	130.28
$\alpha = \beta = \gamma$	90.00	90.00	90.00
Resolution (Å)	91.29-2.20	20.0-2.15	74.95-1.50
Average I/σ(I)[a]	22.5 (11.5)	7.1 (3.4)	17.7 (2.4)
No. unique reflections	39212	41406	120833
Redundancy of reflections[a]	6.0 (6.2)	5.2 (5.5)	6.5 (3.7)
R_{sym}[a,b]	0.06 (0.15)	0.16 (0.50)	0.08 (0.43)
Completeness (%)[a]	100.0 (100.0)	98.0 (99.8)	100.0 (100.0)
Final refinement parameters			
Resolution (Å)	40-2.20	20-2.15	50-1.50
No. of reflections	37234	39316	115715
No. of reflections used for R$_{\text{free}}$ calculation	1967	2089	6117
R$_{\text{cryst}}$,[c] R$_{\text{free}}$ value (%)	15.2, 18.4	21.0, 26.6	16.0, 18.6
Mean *B*-factors (Å^2)	7.8	13.3	16.2
B value from Wilson plot	23.5	24.4	17.2
Residues in most favorable regions (%)[d]	95.0	93.8	94.9
Residues in additionally allowed regions (%)[d]	5.0	6.2	5.1
Root mean square deviation bond length (Å)	0.016	0.019	0.012
Root mean square deviation bond angles (degree)	1.428	1.759	1.405
Protein Data Bank entry	2J2C	2JCM	2JC9

[a] Numbers in parentheses are for the highest resolution shell.
[b] $R_{\text{sym}} = \sum_{hkl}\sum_i |I_i(hkl)| - \langle I(hkl)\rangle|/\sum_{hkl}\sum_i I_i(hkl)$ for *n* independent reflections and observations of a given reflection, $\langle I(hkl)\rangle$ is the average intensity of the *i* observations.
[c] $R_{\text{cryst}} = \sum_{hkl}|F_o(hkl) - F_c(hkl)|/\sum_h |F_o(hkl)|$.
[d] Ramachandran plots are made using PROCHECK Validation (52).
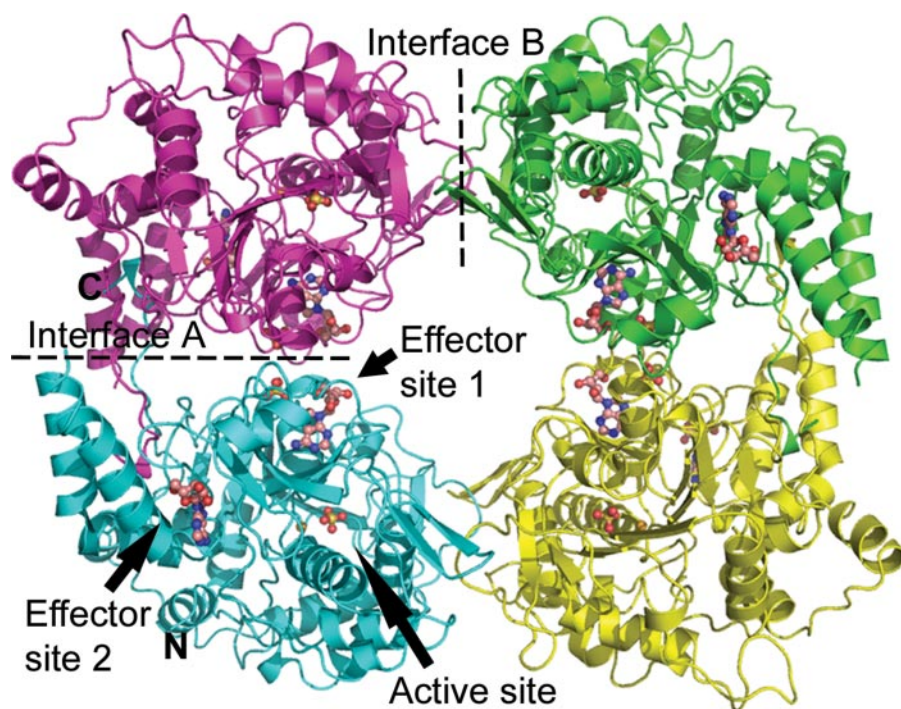
FIGURE 1. **Tetrameric structure of cN-II.** The active site, the effector sites 1 and 2, and the subunit interfaces A and B are pointed out. Sulfates (*red* and *yellow*), magnesium (*orange*), and two adenosines (*white*) are shown. Polar atoms are color-coded as following: nitrogen in *blue* and oxygens in *red*.

pray ionization-mass spectroscopy) reveals a mass of 63.87 kDa, which confirms the identity of the purified construct.

Crystallization and Data Collection—Sitting drop vapor diffusion was used to produce the cN-II crystals by making drops of 1:1 protein:reservoir solution. The crystal used for the native 2.2 Å structure was grown in a 0.2 μl drop at 4 °C for 1 week, with a reservoir solution consisting of 1.8 M of MgSO$_4$ and 0.1 M of Tris, pH 8.5. The crystals that gave the BeF$_3$ and adenosine complexes were grown in 2-μl drops at 4 °C for 1 week. The crystals used for data collection were ~0.2 × 0.2 × 0.3 mm. The crystals were transferred to a 10-μl drop of cryo solution containing 80% (v/v) reservoir solution and 20% (v/v) glycerol for 10–20 s and subsequently flash-frozen in liquid N$_2$. Before cryoprotection, the crystal used for the BeF$_3$ complex was soaked for 45 min in 10 mM BeCl$_2$ and 50 mM NaF, and the crystal used for the adenosine complex was soaked for 90 min in reservoir solution saturated with adenosine. The native data set was collected on beamline ID29 at the European Synchrotron Radiation Facility. Both the BeF$_3$ and the adenosine complexes were collected at beam-line ID14.4 at European Synchrotron Radiation Facility. The data sets of the native structure and the adenosine complex were processed using the programs MOSFLM, version 6.2.5 (35) and SCALA (36), and the data set of the BeF$_3$ complex was processed using XDS and XSCALE (37) (Table 1).

Phasing, Model Building, and Refinement—The structure of cN-II was solved with one polypeptide per asymmetric unit by molecular replacement using the structure of the 31% sequence
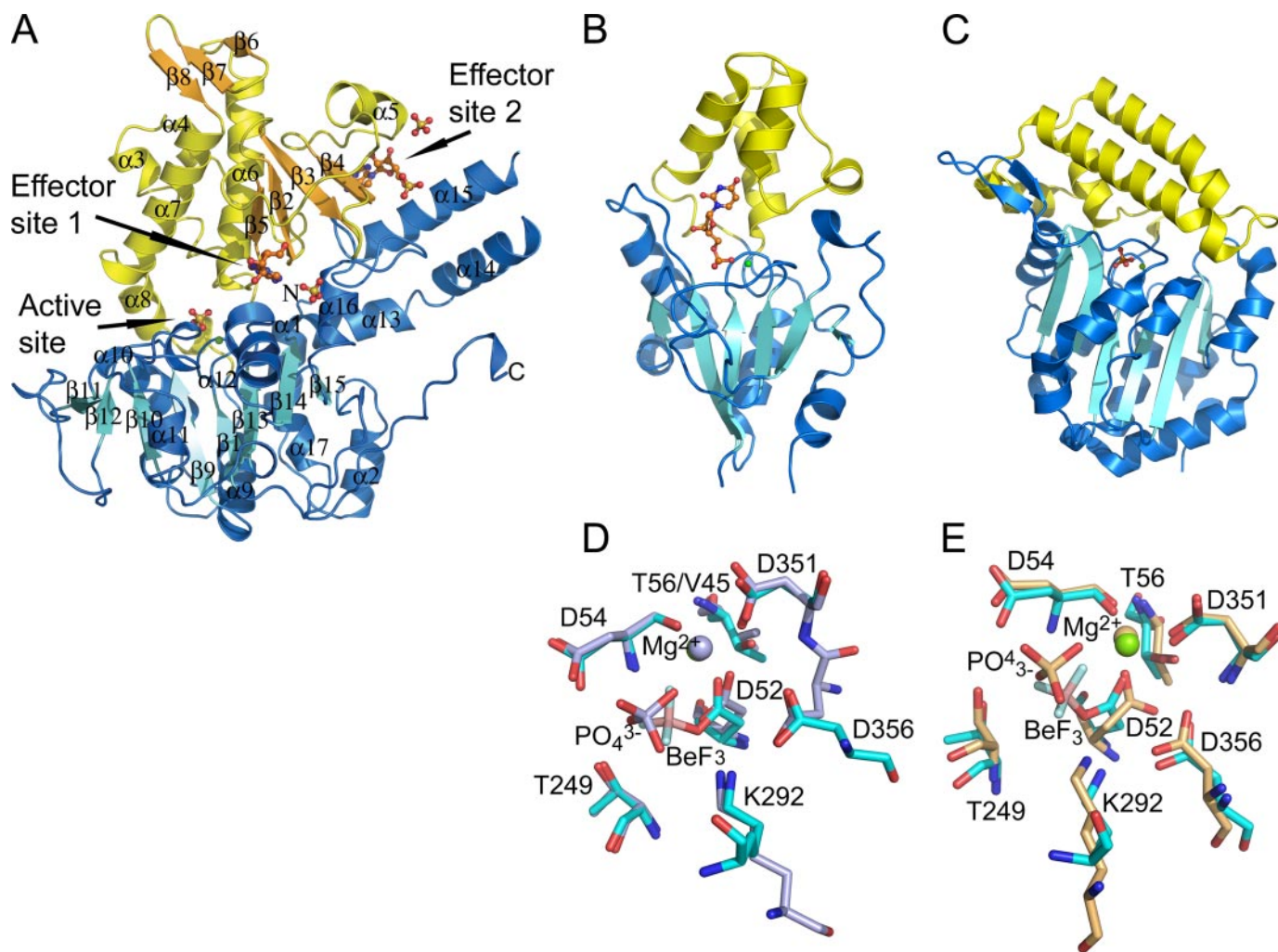
FIGURE 2. **Overall structure of cN-II and comparisons with mdN and cN-III.** *A*, overall structure of cN-II with bound sulfates (*red* and *yellow*), magnesium (*green*), and adenosines (*orange*) with the cap domain in *yellow* and *orange* and the core domain in *blue* and *turquoise*. Secondary structure elements are numbered and marked α for α-helixes and β for β-strands. *B*, overall structure of D41N variant of mdN with dUMP (*orange*) and magnesium (*green*) bound in the active site (PDB entry 1Z4I). *C*, overall structure of mouse cN-III with bound phosphate (*orange*) and magnesium (*green*) in the active site (PDB entry 2G09). *D*, superposition of active sites of cN-II (*turquoise*) in complex with BeF$_3$ (*light blue*) and mdN (*light purple*) in complex with phosphate. The numbers of the residues are those of cN-II. *E*, superposition of active sites of cN-II (*turquoise*) in complex with BeF$_3$ (*light blue*) and mouse cN-III (*light orange*) in complex with phosphate (PDB entry 2G09). Polar atoms are color-coded as following: nitrogen in *blue* and oxygens in *red*. The numbers of the residues are those of cN-II.

identical cN-II from *Legionella pneumophila* (PDB entry 2BDE) as template structure. Phaser (38) was used for molecular replacement, and ARP/wARP (39) was used to finish the initial model and to place solvent molecules. Repeated rounds of manual model building using Coot (40) and translation-libration-screw (TLS) refinement with 10 TLS groups using Refmac5.2 (41) gave the final model. The BeF$_3$ and adenosine complexes were solved by molecular replacement with MolRep (version 9.2) (42), using the native structure as template and copying its set of R_{free} reflections. Structural statistics are shown in Table 1.

RESULTS

Overall Structure—We produced several constructs of cN-II in *Escherichia coli* as N-terminal His$_6$ fusions, including the full-length protein, to achieve diffracting crystals. A construct of residues 1–536 (out of 561) was significantly more soluble than the full-length protein and easier to concentrate to the high concentration needed for crystallization. This construct

was crystallized in 1.8 M MgSO$_4$ and 0.1 M Tris at pH 8.5, and the initial structure was determined to a resolution of 2.2 Å and refined to good stereo geometry. The structure was solved with one molecule in the asymmetric unit. Only residues 1–400 and 417–488 could be unambiguously identified during the structure determination processes. The protein forms a tetramer of four crystallographically related subunits (Fig. 1), which is in agreement with observations from gel filtration chromatography and previous studies supporting that the protein functions as a tetramer (12, 16–18).

In the 2.2-Å structure, six tentative phosphate-binding sites have been identified by the presence of phosphate-like electron density. Although we cannot make conclusive distinctions between phosphate and sulfate ions based on the crystallographic information, we have modeled sulfate ions at these sites since the crystallization solution contained 1.8 M sulfate and only 50 mM phosphate. One of the sulfates is located in the active site together with a magnesium ion and three sulfates are bound in effector sites. From crystals soaked with BeCl$_2$ and

NaF, a structure of cN-II in complex with BeF_3 was solved to 2.15 Å, in which the BeF_3 serves as a model for a potential phosphoenzyme intermediate. Similar BeF_3 complexes of mdN and cN-III have previously been studied (3, 4). In the cN-II structure BeF_3 replaces the sulfate ion found in the active site of the 2.2-Å structure. The 1.5-Å structure of cN-II in complex with two adenosines indicates how the adenosine moiety of the effectors ATP, dATP, ADP, and Ap4A might bind. In this structure the sulfates close to the adenosines are bound at similar sites as in the native 2.2-Å structure.

cN-II has an α/β-domain containing an eight-stranded antiparallel β-sheet surrounded by eight α-helixes, similar to the α/β-Rossmann- like "core domain" seen in mdN, cN-III and other HAD superfamily proteins (Fig. 2, *A*–*C*). The core domain contains the binding site for the phosphate of the substrate nucleotide. Compared with mdN and cN-III, the core domain of cN-II contains five additional α-helixes (α2, α13,

FIGURE 3. **Aligned conserved motifs of the six known intracellular human 5′-nucleotidases mdN, cytosolic 5′(3′)-deoxyribonucleotidase (*cdN*), cytosolic 5′-nucleotidase IA (*cN-IA*), cytosolic 5′-nucleotidase IB (*cN-IB*), cN-II, and cN-III.** Completely conserved residues are shown on *black background*, and partly conserved residues are *boxed*.

α14, α15, α16) and some loop structures involved in subunit interactions or effector binding (Fig. 2*A*). cN-II has also a smaller domain that contains a 4-helix bundle, similar to the "cap domain" that in mdN and cN-III binds the base of the nucleotide (3, 9). This domain is extended to contain also two antiparallel β-sheets consisting of three (β6, β7, and β8) and four (β2, β3, β4, and β5) β-strands, one additional α-helix (α5), and two loop structures participating in effector binding or subunit interaction (Fig. 2*A*).

The tetrameric enzyme consists of two identical dimers in which the sulfates bound in effector site 1 mediate subunit-subunit contacts at interface A (Figs. 1 and 5*B*). Interface A contains 53 residues, of which 19 form hydrogen bonds and 4 form salt bridges with residues of the adjacent subunit. The salt bridges occur between Arg[363] and Asp[145] and between Arg[442] to Glu[487] (Fig. 5*B*). Interface B, which holds the two dimers together (Fig. 1), contains 28 residues, of which 8 make hydrogen bonds. No salt bridges were found at this interface. The subunits are related by 180° rotations around interfaces A and B.

Active Site—The active site of cN-II is located between the core domain and the cap domain as in mdN and cN-III (Fig. 2, *A*–*C*). The core domain contains the conserved Motif I (D*X*D*X*[T/V]L), Motif II ([T/S]) and Motif III (K(X_x)D(X)$_{0-4}$D) that build up the binding site for the phosphate moiety of the substrate and constitute the catalytic machinery in 5′-nucleotidases and most HAD superfamily enzymes (Fig. 3). In cN-II, Motif I consists of Asp[52], Asp[54], Thr[56], and Leu[57], Motif II of Thr[249], and Motif III of Lys[292], Asp[351], and Asp[356]. Fig. 2, *D*–*E*, shows that these residues are structurally conserved compared with mdN and cN-III. Residues Asp[52], Asp[54], Lys[292], and Asp[351] that are directly involved in the proposed nucleotidase reaction mechanism (3) are completely conserved among cN-II, mdN and cN-III, indicating that all three 5′-nucleotidases function by the same mechanism. In line with the previously proposed mechanism for mdN, Asp[52] most likely makes a nucleophilic attack on the phosphate moiety of the substrate forming a pentavalent intermediate (3), whereafter Asp[54] donates a proton to the departing nucleoside (3, 43). Thr[56], which replaces Val[45] of mdN, might be a determinant for the phosphotransferase reaction, see "Discussion." Fig. 4 shows a detailed view over the active site of cN-II with BeF_3 covalently bound to Asp[52], *i.e.* the first Asp of Motif I, similar to what was previously seen in mdN and cN-III (3, 4).

Regulatory Sites—Two effector sites could be characterized from the 1.5-Å structure of cN-II in complex with two adenosines. In effector site 1, an adenosine binds in a well ordered manner with full occupancy (Fig. 5*A*). It forms hydrogen bonds with Gln[453], Asn[154], and several water molecules and is stacked between Phe[354] and Ile[152] (Fig. 5*A*). A sulfate ion interacts with Arg[456] and Arg[144] (Fig. 5*A*) and is located near the 5′-hydroxyl group of adenosine indicating that this could con-
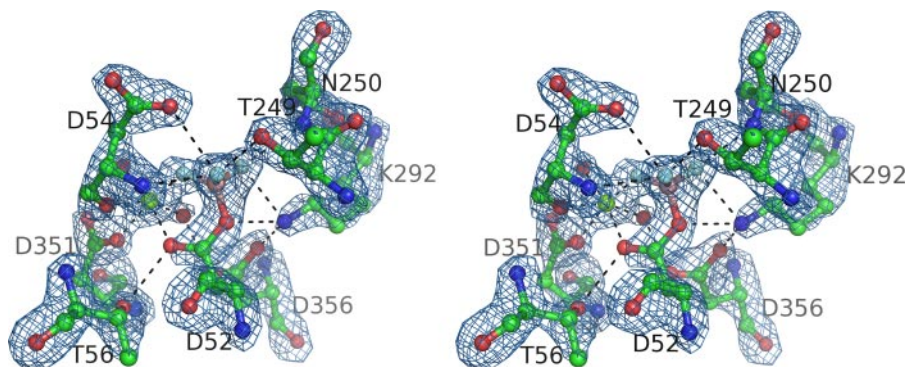

FIGURE 4. **Active site of cN-II with BeF_3 (*light blue*) covalently linked to Asp[52], magnesium (*green*), waters (*red*), and surrounding residues (*green*).** An $F_o - F_c$ omit map with σ level of 4 covers shown residues and ligands. Polar atoms are color-coded as follows: nitrogen in *blue* and oxygens in *red*.
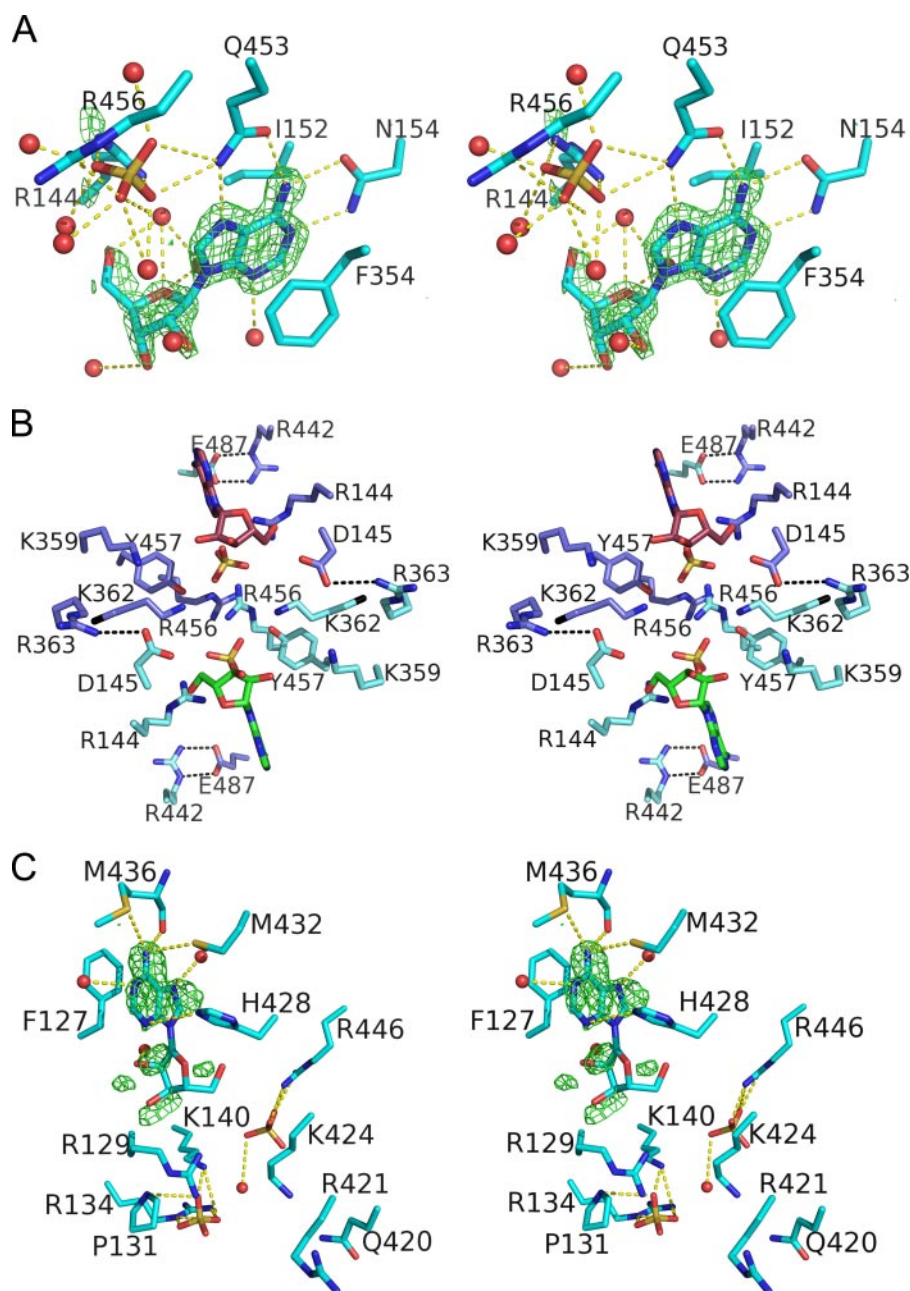
FIGURE 5. **Effector sites 1 and 2 of cN-II with bound adenosine and sulfate.** Omit $F_o − F_c$ maps are covering adenosine with σ level of 4.5 in effector site 1 and σ level of 3 in effector site 2. *A*, stereo image of adenosine bound in effector site 1, with adenosine and amino acid residues colored in *turquoise*. *B*, stereo image of effector site 1 from two adjacent subunits connected through interface A. Salt bridges are indicated by the *dotted lines*. Nitrogens are shown in *blue*, oxygens in *red*, and sulfur in *yellow*. *C*, stereo image of adenosine bound in effector site 2. Note that the ribose moiety is disordered so that the electron density cannot confirm its location. Waters are colored in *red*. Polar atoms are color-coded as following: nitrogen in *blue*, oxygens in *red*, and sulfur in *yellow*.

ordered, the electron density clearly indicates the location of the adenine base (Fig. 5*C*) that forms hydrogen bonds with His[428], Met[432], and Met[436] and two water molecules. The purine ring is stacked between Phe[127] and His[428] (Fig. 5*C*). The nearby residues Arg[129], Arg[131], Arg[134], Arg[446], and Lys[140], which are coordinating sulfate ions (Fig. 5*C*), might coordinate phosphate moieties of adenine nucleotide effectors bound in this site. No significant structural changes can be observed in effector sites 1 and 2 relative to the native structure of the enzyme. Possibly the high sulfate concentration present in the crystallization solution drives the protein into the "effector-bound" conformation, since sulfates might stabilize similar subunit-subunit contacts as effector phosphates.

DISCUSSION

Phosphotransferase Reaction—The detailed molecular mechanism of the phosphotransferase reaction where a phosphate product of the nucleotidase reaction is transferred to a nucleoside acceptor to form a nucleoside monophosphate has not been elucidated yet (22). Of the 5′-nucleotidases, only cN-II and cN-III possess phosphotransferase activity (1). Sequence alignments reveal that both cN-II and cN-III have a Thr in Motif I, whereas all other nucleotidases have a Val at this position (Fig. 3). This suggests that Thr of Motif 1 may be important for the phosphotransferase reaction. In apparent contradiction, it was claimed that cdN isolated from human erythrocytes that lacks the strategic Thr has phosphotransferase activity (44). However, this appears unlikely as cdN isolated

stitute a phosphate-binding site of an adenine nucleotide. Effector site 1 is located near subunit interface A, close to the corresponding site of the adjacent subunit (Fig. 1). Hence the sulfate ions from adjacent subunits bind close to each other, and residues Arg[144], Arg[456], Lys[362], and Tyr[457] from the two subunits together form a large pocket where the phosphates of adenine nucleotides might bind at the interface between the subunits (Fig. 5*B*).

In effector site 2 a second adenosine binds in a much less ordered manner. Whereas the ribose moiety is completely dis-

from human placenta and recombinant murine cdN did not show this activity (45, 46).

In murine cN-III three different conformations of the first Asp in Motif I have been reported (4). In a 2.1-Å structure of the enzyme in complex with phosphate (PDB entry 2G09) (4), the catalytic Asp has flipped so that the nucleophilic carboxyl oxygen forms a tight (2.6 Å) hydrogen bond with the Thr (Fig. 2*E*). The same occurs in our structure of human cN-III in complex with phosphate solved to 3.0 Å (PDB entry 2JGA). Most likely the flipped Asp conformation is not possible when a Val substi-
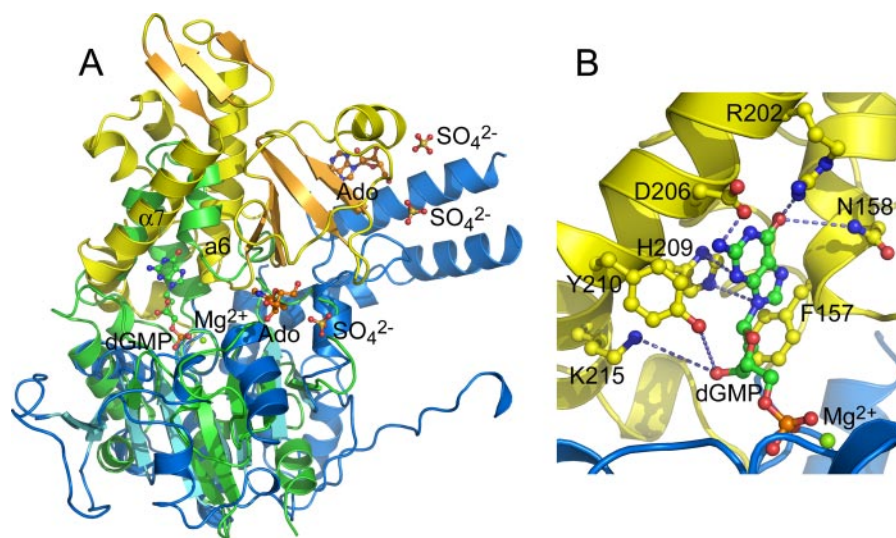
FIGURE 6. **Substrate recognition in cN-II shown by the superposition of cN-II on mdN in complex with dGMP (9).** *A*, overall structures of cN-II and mdN superposed. The mdN structure with dGMP bound is shown in *green* and the cN-II structure is shown in *yellow*, *orange*, *blue*, and *turquoise*. *B*, zoom-in on the active site with dGMP (*green*) of the mdN structure indicating which residues of cN-II (*yellow* and *blue*) are involved in substrate binding.
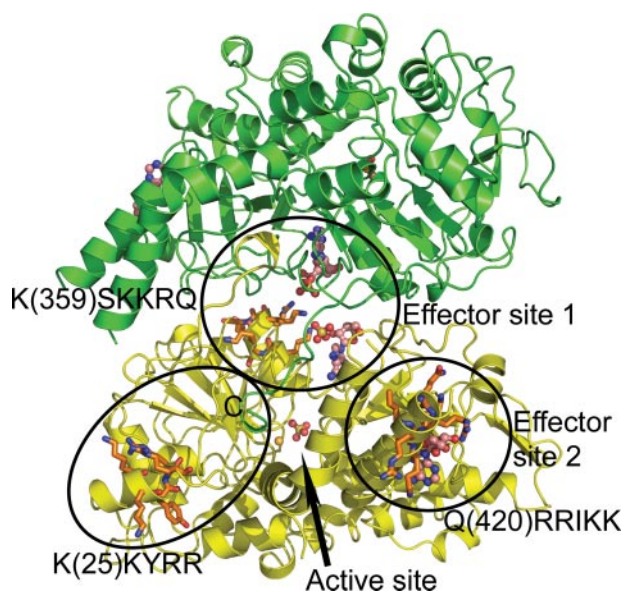

FIGURE 7. **Two subunits of the tetrameric cN-II with three positively charged regions (K(25)KYRR), (K(359)SKKRQ), and (Q(420)RRIKK) shown in *orange*.** Adenosines (*white*), sulfates (*yellow* and *red*), and magnesium (*yellow*) are also shown. Nitrogens are shown in *blue* and oxygens in *red*. The C-terminal end of the structure (residue 488) is marked *C*.

tutes the Thr as in mdN, cdN, cN-IA and cN-IB, since the Asp would be repelled by the hydrophobic Val. The phosphotransferase reaction might require the flexibility of the Asp nucleophile but the exact cause for this requirement is not clear from the structures. In the phosphotransferase reaction it is the 5′-hydroxyl group of the nucleoside acceptor that makes the nucleophilic attack on the phosphate. The activation of the 5′-hydroxyl group for this reaction will require a general base that can take up the 5′-hydroxyl proton. In uridine-cytidine kinase 2, which phosphorylates uridine and cytidine in the UTP and CTP salvage pathway, an Asp probably acts as the general base (47). In cN-II, Asp[54], which is proposed to serve as

a base and activate a water molecule in the nucleotidase reaction (3), could have this role also for the phosphotransferase reaction. This suggests that also the phosphotransferase reaction will include a phosphoenzyme intermediate and that the donating and accepting nucleotides will occupy similar binding sites in a sequential binding scenario.

Substrate Recognition—Soakes with nucleotides did not yield binding in the active site, presumably due to the presence of bound sulfate. However, by superposing the structure of cN-II on the previously solved structure of mdN in complex with dGMP (9) we can identify residues that are likely to be involved in substrate recognition. Fig. 6*A* shows that in the cap domain the two α-helices (α6 and α7) that take part in binding of the substrate base, overlap between cN-II and mdN, although the interacting residues are not conserved. The direct superposition of mdN-bound dGMP suggests the interactions that might mediate the recognition of dGMP/GMP in the active site of cN-II (Fig. 6, *A* and *B*). This modeling suggests that Asp[206] binds the amino group of guanine, Arg[202] and Asn[158] the 6-carbonyl group and His[209] at least one of the electronegative nitrogen groups (Fig. 6*B*). Phe[157] probably stacks to non-polar parts of the substrate nucleotide and Tyr[210] and Lys[215] bind the 2′- and 3′-hydroxyl groups of the ribose. The specificity of the enzyme for 6-hydroxypurine nucleotides may depend on Arg[202] and Asn[158] that hinder the binding of dAMP/AMP.

Regulation—The cN-II has a stretch of 13 Asp/Glu residues at the C-terminal, which might be involved in subunit association/dissociation (16). Elimination of these 13 residues gave 20-fold decreased expression, changed the normally tetrameric protein into a monomer, and gave a 2-fold increase in K_m and a 20-fold decrease of specific activity (16). Our construct, which lacks 25 C-terminal residues, showed high expression level and runs as a tetramer on gel filtration. The same occurred with a construct of residues 30–549 (lacking 12 C-terminal residues). These observations suggest that the protein lacking the 13 C-terminal residues might have been misfolded, possibly because a different expression system were used than in this study (16). Three positively charged regions, (K(25)KYRR), (K(359)SKKRQ), and (Q(420)RRIKK) were suggested as possible interaction partners for the acidic C-terminal stretch (16). The present structure suggests that (K(359)SKKRQ) and (Q(420)RRIKK) take part in binding phosphate moieties of effectors at effector site 1 and 2, respectively, thus (K(25)KYRR) remains the most likely candidate for binding the C-terminal acidic stretch (Fig. 7).

The cN-II is allosterically activated by dATP, ATP and ADP, 2,3-BPG, and purine dinucleoside polyphosphates such as Ap4A. Of the diadenosine polyphosphates (Ap(n)A), only those containing 4–6 phosphates are activators, while neither Ap3A
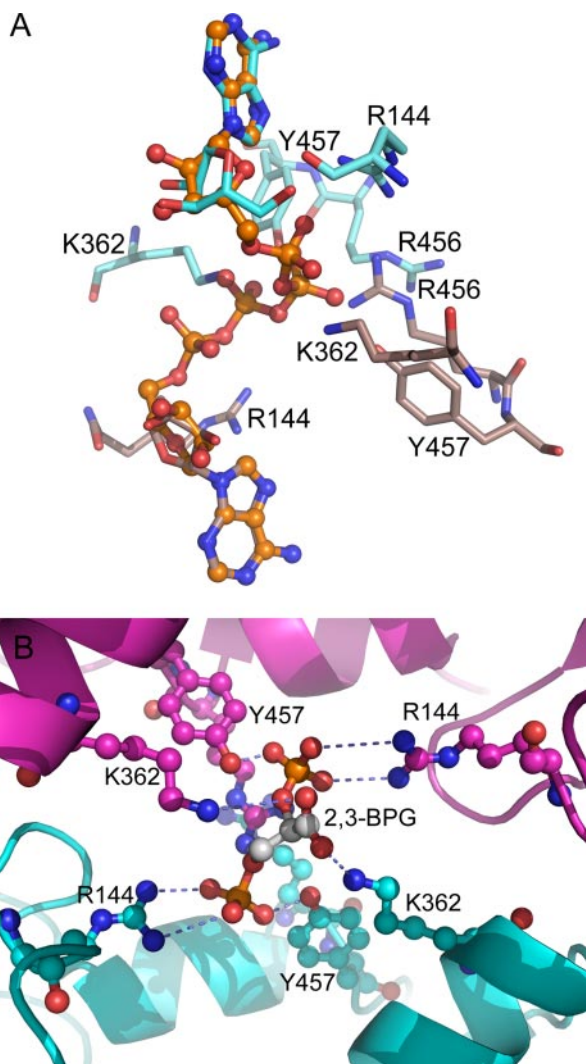
FIGURE 8. **The effectors Ap4A and 2,3-BPG modeled in effector site 1.** *A*, modeled Ap4A (*orange*) superimposed on cN-II in complex with adenosine. Two adjacent subunits are distinguished by color (*blue* and *brown*). The adenosine moieties of Ap4A fit nicely in the adenosine sites, as indicated by the excellent superposition on the adenosines determined experimentally. *B*, effector site 1 with 2,3-BPG, modeled between two adjacent subunits.

nor Ap2A can activate the enzyme (18). Diadenosine polyphosphates have been proposed as intracellular and extracellular signaling molecules in animal cells (48). Ap3A and Ap4A have opposite behavior during cell differentiation and apoptosis in human cells (49, 50) with Ap4A levels increasing and Ap3A levels decreasing during apoptosis (49).

Activation of cN-II by Ap4A during apoptosis might stimulate the catabolism of purine nucleotides originated from degradation of DNA and RNA and make the resulting membrane-permeable nucleosides available to other cells and tissues.

At effector site 1 located near subunit interface A (Fig. 1), we modeled Ap4A between two subunits with one adenosine moiety in each subunit (Fig. 8*A*). These interactions efficiently glue the tetramer subunits together in pairs and suggest the modulation of subunit association to be the base of the activation induced by effectors at effector site 1. Modeling suggests that Ap4A fits nicely in effector site 1 with the phosphates coordinated by positive residues (Fig. 8*A*), while Ap3A has too short a

phosphate chain to permit a favorable binding of the adenosines in the adenosine sites. This may explain how cN-II discriminates between Ap4A and Ap3A.

We have also modeled 2,3-BPG in effector site 1 with the phosphates in the sulfate density found in effector site 1, one in each subunit (Fig. 8*B*). Similarly to Ap4A, 2,3-BPG mediates subunit contacts at interface A. As modeled, the 2,3-BPG interacts favorably with Lys[362], Tyr[457], and Arg[144] from both subunits. This favorable binding surface indicates that this is a likely binding site for 2,3-BPG.

The adenosine-bound structure suggests that cN-II has at least two unique effector sites for adenine-based nucleotides, and that Ap4A and 2,3-BPG might bind in effector site 1. Two active forms of cN-II were isolated from calf thymus (51). The 59-kDa form A appeared to contain two effector sites, one for ATP and ADP and one for 2,3-BPG, while the 54-kDa form B contained three separate effector sites for ATP, ADP, and 2,3-BPG (51). In form A no synergy was observed between the activators, whereas ADP and ATP acted synergistically on form B (51). Our construct with its two effector sites may correspond to form B. We cannot rule out that 2,3-BPG can bind in effector site 1 at the same time as a nucleotide, which would imply a separate effector site for 2,3-BPG (51).

In conclusion the present structure reveals possible structural determinants for the phosphotransferase reaction and for the binding of substrate and regulators to cN-II. However, further structural studies of cN-II in complex with substrates, with and without effectors, is required to reveal the detailed mechanism for allosteric regulation. The regulatory sites identified in the present structure may provide useful information for the design of compounds that selectively modulate or inhibit the activity of cN-II leaving the other 5′-nucleotidases unaffected. The targeting of the allosteric sites of cN-II might therefore be an avenue to reduce drug resistance against nucleoside analogs and the neurological symptoms related to the Lesch-Nyhan syndrome.

REFERENCES

1. Hunsucker, S. A., Mitchell, B. S., and Spychala, J. (2005) *Pharmacol. Ther.* **107,** 1–30
2. Bianchi, V., and Spychala, J. (2003) *J. Biol. Chem.* **278,** 46195–46198
3. Rinaldo-Matthis, A., Rampazzo, C., Reichard, P., Bianchi, V., and Nordlund, P. (2002) *Nat. Struct. Biol.* **9,** 779–787
4. Bitto, E., Bingman, C. A., Wesenberg, G. E., McCoy, J. G., and Phillips, G. N. (2006) *J. Biol. Chem.* **281,** 20521–20529
5. Wang, W., Kim, R., Jancarik, J., Yokota, H., and Kim, S. H. (2001) *Structure (Lond.)* **9,** 65–71
6. Collet, J. F., Stroobant, V., Pirard, M., Delpierre, G., and Van Shaftingen, E. (1998) *J. Biol. Chem.* **273,** 14107–14112
7. Lahiri, S. D., Zhang, G. F., Dunaway-Mariano, D., and Allen, K. N. (2003) *Science* **299,** 2067–2071
8. Allegrini, S., Scaloni, A., Ferrara, L., Pesi, R., Pinna, P., Sgarrella, F., Camici, M., Eriksson, S., and Tozzi, M. G. (2001) *J. Biol. Chem.* **276,** 33526–33532
9. Wallden, K., Ruzzenente, B., Rinaldo-Matthis, A., Bianchi, V., and Nordlund, P. (2005) *Structure (Lond.)* **13,** 1081–1088
10. Itoh, R., Mitsui, A., and Tsushima, K. (1967) *Biochim. Biophys. Acta* **146,** 151–156

11. Bretonnet, A. S., Jordheim, L. P., Dumontet, C., and Lancelin, J. M. (2005) *FEBS Lett.* **579,** 3363–3368
12. Spychala, J., Madrid-Marina, V., and Fox, I. H. (1988) *J. Biol. Chem.* **263,** 18759–18765
13. Pesi, R., Turriani, M., Allegrini, S., Scolozzi, C., Camici, M., Ipata, P. L., and Tozzi, M. G. (1994) *Arch. Biochem. Biophys.* **312,** 75–80
14. Allegrini, S., Pesi, R., Tozzi, M. G., Fiol, C. J., Johnson, R. B., and Eriksson, S. (1997) *Biochem. J.* **328,** 483–487
15. Randitelli, S., Baiocchi, C., Pesi, R., Allegrini, S., Turriani, M., Ipata, P. L., Camici, M., and Tozzi, M. G. (1996) *Int. J. Biochem. Cell Biol.* **28,** 711–720
16. Spychala, J., Chen, V., Oka, J., and Mitchell, B. S. (1999) *Eur. J. Biochem.* **259,** 851–858
17. Itoh, R. (1993) *Comp. Biochem. Physiol. B Biochem. Mol. Biol.* **105,** 13–19
18. Marques, A. F. P., Teixeira, N. A., Gambaretto, C., Sillero, A., and Sillero, M. A. G. (1998) *J. Neurochem.* **71,** 1241–1250
19. Oka, J., Matsumoto, A., Hosokawa, Y., and Inoue, S. (1994) *Biochem. Biophys. Res. Commun.* **205,** 917–922
20. Rampazzo, C., Gazziola, C., Ferraro, P., Gallinaro, L., Johansson, M., Reichard, P., and Bianchi, V. (1999) *Eur. J. Biochem.* **261,** 689–697
21. Pinto, R. M., Canales, J., Sillero, M. A. G., and Sillero, A. (1986) *Biochem. Biophys. Res. Commun.* **138,** 261–267
22. Worku, Y., and Newby, A. C. (1982) *Biochem. J.* **205,** 503–510
23. Johnson, M. A., and Fridland, A. (1989) *Mol. Pharmacol.* **36,** 291–295
24. Tozzi, M. G., Camici, M., Pesi, R., Allegrini, S., Sgarrella, F., and Ipata, P. L. (1991) *Arch. Biochem. Biophys.* **291,** 212–217
25. Carson, D. A., Carrera, C. J., Wasson, D. B., and Iizasa, T. (1991) *Biochim. Biophys. Acta* **1091,** 22–28
26. Schirmer, M., Stegmann, A. P. A., Geisen, F., and Konwalinka, G. (1998) *Exp. Hematol.* **26,** 1223–1228
27. Lotfi, K., Mansson, E., Chandra, J., Wang, Y. Y., Xu, D. W., Knaust, E., Spasokoukotskaja, T., Liliemark, E., Eriksson, S., and Albertioni, F. (2001) *Br. J. Haematol.* **113,** 339–346
28. Galmarini, C. M., Thomas, X., Graham, K., El Jafaari, A., Cros, E., Jordheim, L., Mackey, J. R., and Dumontet, C. (2003) *Br. J. Haematol.* **122,** 53–60
29. Yamamoto, S., Yamauchi, T., Kawai, Y., Takemura, H., Kishi, S., Yoshida, A., Urasaki, Y., Iwasaki, H., and Ueda, T. (2007) *Int. J. Hematol.* **85,** 108–115
30. Mazzon, C., Rampazzo, C., Scaini, M. C., Gallinaro, L., Karlsson, A., Meier, C., Balzarini, J., Reichard, P., and Bianchi, V. (2003) *Biochem. Pharmacol.* **66,** 471–479
31. Wu, J. Z., Larson, G., Walker, H., Shim, J. H., and Hong, Z. (2005) *Antimicrob. Agents Chemother.* **49,** 2164–2171
32. Pesi, R., Micheli, V., Jacomelli, G., Peruzzi, L., Camici, M., Garcia-Gil, M., Allegrini, S., and Tozzi, M. G. (2000) *Neuroreport* **11,** 1827–1831
33. Garcia-Gil, M., Pesi, R., Perna, S., Allegrini, S., Giannecchini, M., Camici, M., and Tozzi, M. G. (2003) *Neuroscience* **117,** 811–820
34. Ericsson, U. B., Hallberg, B. M., DeTitta, G. T., Dekker, N., and Nordlund, P. (2006) *Anal. Biochem.* **357,** 289–298
35. Leslie, A. G. W. (1992) *Joint CCP4 & ESF-EAMCB Newsletter on Protein Crystallography*, No. 26
36. Kabsch, W. (1988) *J. Appl. Crystallogr.* **21,** 916–924
37. Kabsch, W. (1988) *J. Appl. Crystallogr.* **21,** 67–71
38. Read, R. J. (2001) *Acta Crystallogr. Sect. D Biol. Crystallogr.* **57,** 1373–1382
39. Perrakis, A., Morris, R., and Lamzin, V. S. (1999) *Nat. Struct. Biol.* **6,** 458–463
40. Emsley, P., and Cowtan, K. (2004) *Acta Crystallogr. Sect. D Biol. Crystallogr.* **60,** 2126–2132
41. Murshudov, G. N., Vagin, A. A., and Dodson, E. J. (1997) *Acta Crystallogr. Sect. D Biol. Crystallogr.* **53,** 240–255
42. Vagin, A., and Teplyakov, A. (1997) *J. Appl. Crystallogr.* **30,** 1022–1025
43. Himo, F., Guo, J. D., Rinaldo-Matthis, A., and Nordlund, P. (2005) *J. Phys. Chem. B* **109,** 20004–20008
44. Amici, A., Emanuelli, M., Magni, G., Raffaelli, N., and Ruggieri, S. (1997) *FEBS Lett.* **419,** 263–267
45. Rampazzo, C., Johansson, M., Gallinaro, L., Ferraro, P., Hellman, U., Karlsson, A., Reichard, P., and Bianchi, V. (2000) *J. Biol. Chem.* **275,** 5409–5415
46. Hoglund, L., and Reichard, P. (1990) *J. Biol. Chem.* **265,** 6589–6595
47. Suzuki, N. N., Koizumi, K., Fukushima, M., Matsuda, A., and Inagaki, F. (2004) *Structure (Lond.)* **12,** 751–764
48. Kisselev, L. L., Justesen, J., Wolfson, A. D., and Frolova, L. Y. (1998) *FEBS Lett.* **427,** 157–163
49. Vartanian, A., Prudovsky, I., Suzuki, H., DalPra, I., and Kisselev, L. (1997) *FEBS Lett.* **415,** 160–162
50. Vartanian, A. A., Suzuki, H., and Poletaev, A. I. (2003) *Biochem. Pharmacol.* **65,** 227–235
51. Pesi, R., Baiocchi, C., Allegrini, S., Moretti, E., Sgarrella, F., Camici, M., and Tozzi, M. G. (1998) *Biol. Chem.* **379,** 699–704
52. Laskowski, R. A., Macarthur, M. W., Moss, D. S., and Thornton, J. M. (1993) *J. Appl. Crystallogr.* **26,** 283–291

The Journal of Biological Chemistry